Atmospheric Research 166 (2015) 24–32

Contents lists available at ScienceDirect

Atmospheric Research

journal homepage: www.elsevier.com/locate/atmos

Evaluation of the WRF model configuration for Zonda wind events in a complex terrain

S.E. Puliafito [a,b,c], D.G. Allende [a], C.G. Mulena [a,c], P. Cremades [a,c], S.G. Lakkis [d,e]

[a] Grupo de Estudios de la Atmósfera y el Ambiente, Facultad Regional Mendoza, Universidad Tecnológica Nacional (UTN), Rodríguez 273, M5502AJE Mendoza, Argentina
[b] Facultad Regional Buenos Aires, UTN, Medrano 951, Buenos Aires, Argentina
[c] Consejo Nacional de Investigaciones Científicas y Técnicas (CONICET), Argentina
[d] Facultad de Ciencias Agrarias, Pontificia Universidad Católica Argentina (UCA), Cap. Gral. Ramón Freire 183, C1426AVC Buenos Aires, Argentina
[e] Unidad de Investigación y Desarrollo de las Ingenierías (UIDI), Facultad Regional Buenos Aires (FRBA), Universidad Tecnológica Nacional (UTN), Argentina

ARTICLE INFO

Article history:
Received 13 January 2015
Received in revised form 11 June 2015
Accepted 13 June 2015
Available online 23 June 2015

Keywords:
Andes Mountain Range
Model configurations
Mendoza-Argentina
Weather Research and Forecasting
Zonda wind

ABSTRACT

The Weather Research and Forecasting (WRF) model was used to simulate two mesoscale events of Zonda winds that occurred in August 2010 and April 2011. The model was applied on a complex terrain area of high mountains in Mendoza, western Argentina. The WRF numerical model performance was evaluated for two reanalysis datasets and two land use and land cover databases in order to verify the influence of forcing conditions and to find the configuration that best reproduces these severe conditions. Results were evaluated using meteorological data from three surface stations and two stations with radiosondes for the following variables: temperature, dew point, and meridional and zonal winds components. Upper air data were analyzed for standard pressure levels. Results clearly showed a better performance from the locally adapted model in predicting surface variables. Furthermore, distinct tendencies were found with regard to the preferred configuration for upper air variables at different levels of pressure, both in the use of land use and land cover databases and of reanalysis data.

1. Introduction

Zonda is a regional term that is used for high intensity winds that often occur on the western side of the Andes, in the subtropical latitudes of South America. Its origin, closely linked with the topography, has similarities with the Foehn winds in the Alps, between Germany, Austria and Switzerland; the Chinook winds of Canada and the United States, east of the Rocky Mountains or the Berg winds in South Africa. Many authors have described the typical meteorological conditions of these winds in the Northern Hemisphere (Zydek, 2000; Ezcurra et al., 2013; Kaltenboeck and Steinheimer, 2014; Mira-Salama et al., 2008; Sun, 2013). In the Southern Hemisphere, these complex episodes have been studied by Norte (1988), Seluchi et al. (2003) and Viale and Nuñez (2010).

Zonda events often occur along the subtropical Andes, but they are detected with more frequency and intensity near two cities of western Argentina: Mendoza (32.8°S, 68.8°W, and 704 m above sea level) and San Juan (31.5°S, 68.5°W, and 598 m a.s.l.). The high-intensity, high-speed westerly wind prevailing in the area loads the atmosphere with dust due to soil erosion, leading to low visibility and air quality aggravation issues.

Norte (1988) and Seluchi et al. (2003) have defined two categories of Zonda episodes: "high" Zonda and "surface" Zonda. The former occurs when wind is detected at the Eastern slopes of the mountain but not at the plain stations. The latter develops on the eastern side of the Andes, near the cities of Mendoza and San Juan. The events may be classified according to maximum wind gust intensity, as follows: "moderate" (Z1), when wind maximum speeds are less or equal to 35 kt ($\leq$18 m s^{-1}); "severe" (Z2), when the maximum value is equal to or higher than 35 kt (>18 m s^{-1}) and less than 50 kt (<25 m s^{-1}); "very severe" (Z3), if wind maximum gustiness are equal to or higher than 50 kt ($\geq$25 m s^{-1}) and less than 65 kt (<33 m s^{-1}); and "extremely severe or catastrophic" (Z4), when gustiness exceed 65 kt (>33 m s^{-1}).

Zonda characterization may be complemented with satellite images that show trapezoidal or triangular middle clouds in the center of Chile and triangular ones in the Pacific Ocean. However, in order to describe wind intensity and direction with higher resolution or the beginning and end of these events, additional analyses are needed (Norte et al., 2008). Therefore, in order to obtain a reliable prediction of wind flows in complex terrains, an appropriate simulation tool that includes a proper description of the terrain and of land uses is required.

Several regional numerical prediction models have been used for analysis and prediction of Zonda events. For example, i) Eta-CPTEC (Centre for Weather Forecasts and Climate Studies—Brazil) with horizontal resolutions of 40 and 15 km (Seluchi et al., 2003; Mesinger et al., 2006) and ii) the Brazilian Regional Atmospheric Modelling System (BRAMS) with horizontal resolution of 20 km (Norte et al., 2008). The BRAMS model has also been applied to the study of other

E-mail address: epuliafito@frm.utn.edu.ar (S.E. Puliafito).

http://dx.doi.org/10.1016/j.atmosres.2015.06.011
0169-8095/

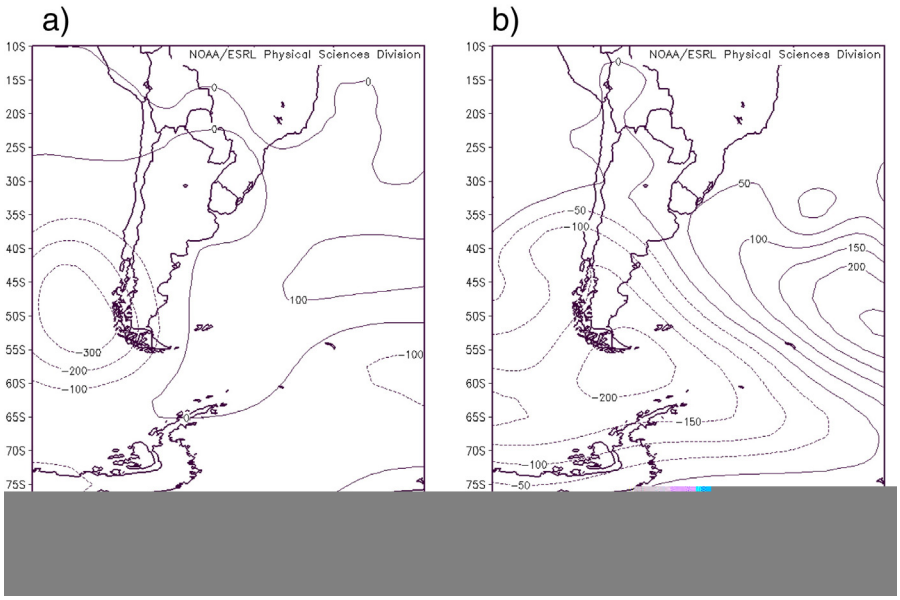

Fig. 1. Geopotential height, composite anomaly, at 500 mb, for April 21st (a) and August, 28th (b).

meteorological phenomena in South America (Borque et al., 2010; Nicolini and García, 2011). In such simulations, the performance of the models used to represent atmospheric dynamics during Zonda periods is variable, with persistent deviations, particularly in variables such as wind speed and direction. These deviations need to be minimized. Several authors highlight the importance of having better spatial

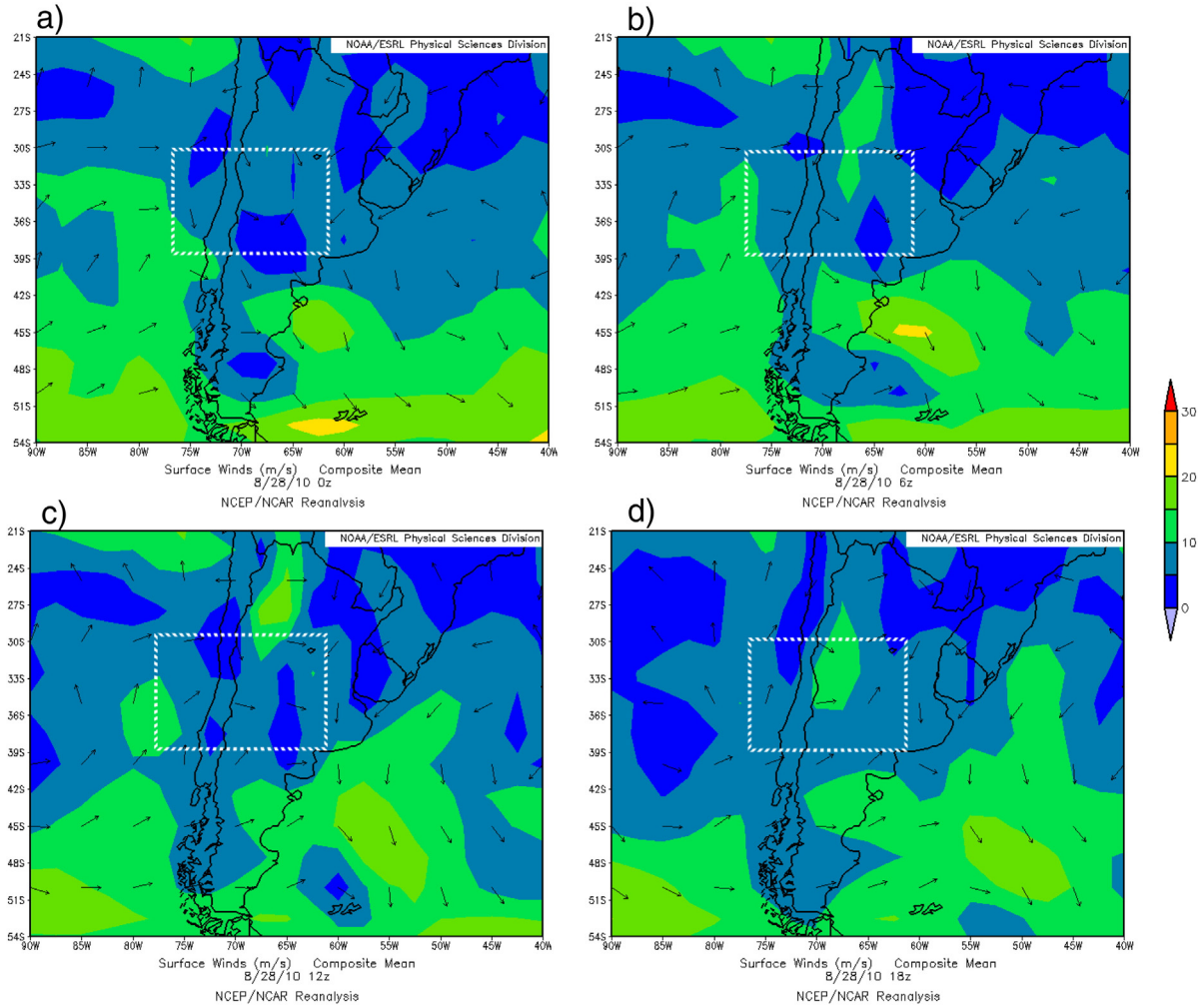

Fig. 2. Wind vectors (Surface reanalysis) in ms^{-1} on August 28, at 0000 UTC (a), 0600 UTC (b), 1200 UTC (c) and 1800 UTC (d).

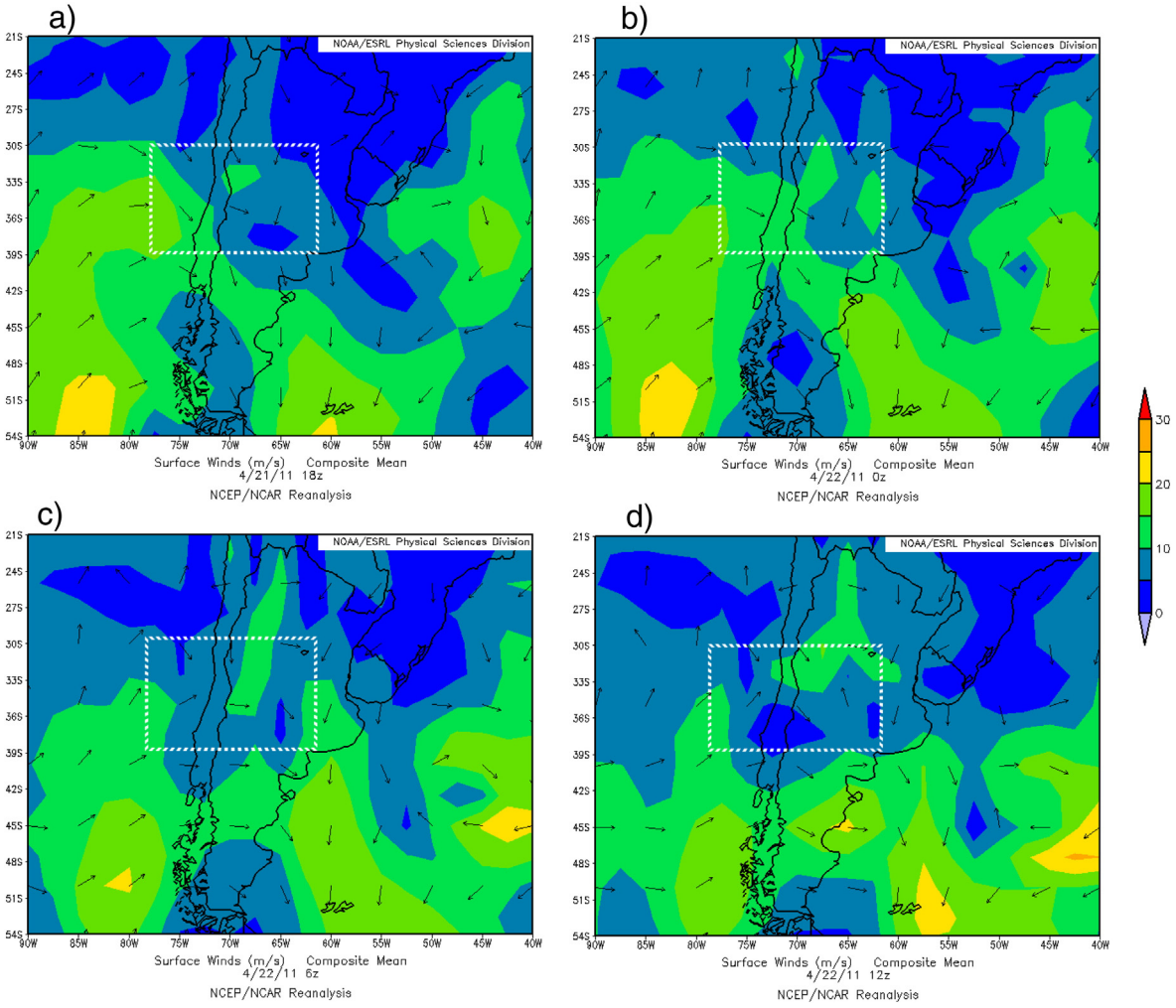

Fig. 3. Wind vectors (Surface reanalysis) in m s^{-1} on April 21, at 1800 UTC (a), and on April 22 at 0000 UTC (b), 0600 UTC (c) and 1800 UTC (d).

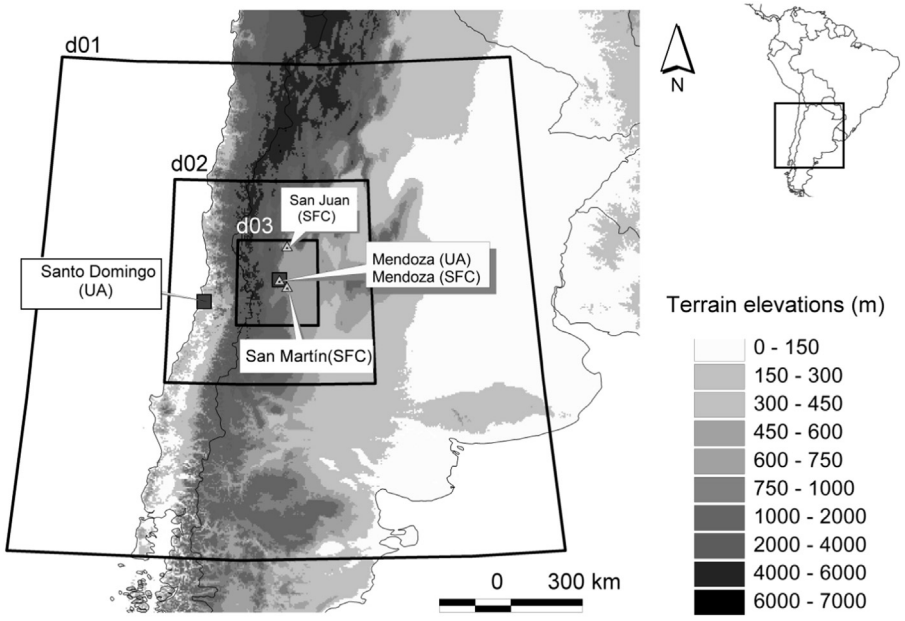

Fig. 4. Modeling domain for Zonda events simulation. The marks indicate the locations of the surface weather stations (SFC) at Mendoza, San Juan and San Martín, and the upper air stations (UA) at Mendoza and Santo Domingo.

Table 1
WRF local configuration.

Parameterization	Schemes	WRF variable	WRF value
Input			
Terrain elevation	SRTM3	–	–
LULC	USGS/GEAA[a]	–	–
Reanalysis	GFS/ERA[a]		
Resolution			
Temporal	Δt (seg)	time_step	90
Spatial	Δx, Δy (km)	dx,dy	36, 12, 4
Vertical	Δz (ETA levels)	e_vert	60 level
Input	Nesting	input_from_file	.T.,.T.,.T.
Physics			
Microphysics	Eta microphysics (operational in NCEP models)	mp_physics	95, 5, 5
Long-wave radiation	RRTM	ra_lw_physics	1, 1, 1
Short-wave radiation	Goddard Dudhia	ra_sw_physics	2, 1, 1
Surface	Noah Land Surface Model: Unified NCEP/NCAR/AFWA	sf_surface_physics	2, 2, 2
Surface levels	–	num_soil_layers	4
Surface layer physics	Monin–Obukhov similarity Theory	sf_sfclay_physics	1, 1, 1
PBL	YSU	bl_pbl_physics	1, 1, 1
Cumulus	Kain–Fritsch scheme	cu_physics	1, 1, 0
Dynamics			
Integration	Runge–Kutta 2nd order	rk_ord	3
Vertical speed	Damping enabled	w_damping	1
Turbulence and mixture	2nd order diffusion	diff_opt	1
Eddy coefficent	Smagorinsky	km_opt	4
Prognostics	Disabled	progn	0
Four dimensional data assimilation			
Analysis nudging	–	grid_fdda	1,1,0
Observational nudging	–	obs_nudge_opt	0,0,0

[a] These are the only configurations that vary in each case study.

resolutions and high quality representation of local factors for better simulations of micro and regional scale circulations (Carvalho et al., 2012; DuVivier and Cassano, 2012; Jiménez et al., 2010; Lee et al., 2015; Papanastasiou et al., 2010; Santos-Alamillos et al., 2015). Consequently, it is expected that a proper description of terrain elevations and a better characterization of land use and cover associated to the Weather Research and Forecasting (WRF) model (Michalakes et al., 2004; Skamarock et al., 2008) will allow a better prediction of wind flows in comparison with Zonda evaluation using only reanalysis data or other numerical models. Furthermore, different approaches to downscaling lead to different estimations of properties in a fine scale.

Therefore, the objectives of this work are: 1) to improve the characterization of the temporal and spatial evolution of temperature, dew point, zonal and meridional wind components during Zonda episodes; 2) to evaluate WRF numerical model performance forced by two reanalysis datasets from ERA Interim (European Reanalysis) and NCEP GFS (National Centre for Environmental Prediction—Global Forecast System), that serve as initial and time-updated lateral meteorological boundary conditions; as well as databases with different land use and land cover (LULC) in order to verify the influence of different modeling approaches and 3) to find the configuration that best reproduces these severe conditions in the mountainous terrain of the Andes Mountain Range. To achieve the above mentioned objectives, two surface Zonda events of different magnitude which occurred in August 2010 and April 2011 were analyzed using the WRF model. The results were evaluated using meteorological data from three surface stations (Mendoza, San Martín and San Juan, in Argentina) and two stations with radiosondes (Mendoza, Argentina and Santo Domingo, Chile) to evaluate upper air information at mandatory pressures levels.

Table 2
Variables, stations and databases used in the comparison.

Parameters	Options
Events	ZA, ZB
Variables	*T*, *DP*, *U10*, *V10*
Reanalysis	GFS, ERA
LULC	USGS, GEAA
Surface stations	Mendoza, San Martín, San Juan
Upper air stations	Mendoza, Santo Domingo
Pressure levels (hPa)	1000, 925, 850, 700, 500, 400, 300, 250, 200, 150, 100
Statistics	MBE, RMSD, RMSE, d-index, disp, BIAS

2. Materials and methods

2.1. Description of events

According to reanalysis data from the NCEP, the Zonda events that occurred on August 28, 2010 (Zonda A: ZA) and on April 21, 2011 (Zonda B: ZB) showed negative anomalies at the geopotential height of 500 mbar or low pressure levels between 50°S and 60°S, indicating the presence of high atmospheric instability which moved forward toward the Andes Mountain Range, from west to south-west (Fig. 1).

Skew-T diagrams obtained for Mendoza, at 1200 UTC for both events, showed a high level of dryness in the middle troposphere and a low dry adiabatic gradient. A closer analysis of synoptic data showed the presence of Zonda with higher temperatures and lower dew point values in the region in comparison with other stations at the same latitude.

On August 28, Zonda (ZA) with a stratified initial evolution of the main flow centered in the study area was detected. The presence of this flow increased the intensity of the Foehn effect. Fig. 2 shows the evolution of the main flow, which on August 28 entered the analysis domain and grew to reach full development. Maximum wind intensity, estimated from surface station observations, reached gusts of 40 km/h. This event may be classified as *severe* according to Norte's description (Norte, 1988).

On August 29, the area under study was no longer under the influence of Zonda winds. Instead, it had weaker winds and the main flow was parallel to the mountain range with higher intensities beyond the study area boundaries.

Zonda's main flow (ZB) of April 21 2011 (Fig. 3) developed strongly on April 19 but it appeared further south of the area of interest. For the following two days, the front of the flow traveled to the central area of study with medium intensity. On April 21, temperature values increased and pressure values decreased at the surface levels. This Zonda event was classified as *moderate*, with wind gusts of up to 16 m s^{-1}, according to the estimations at surface stations. Several hours after the peak of the episode, meteorological values had reached their monthly averages (after 1800 UTC of April 22).

2.2. Modeling approach

The area under study is located in the southern Andes, at the western part of Argentina. Three domains were defined in order to downscale the atmosphere's physical properties (Fig. 4). The largest domain (of 36 km grid cells) centered at 34.1°S, 64.5°W with an area

Table 3
Performance statistics obtained for surface temperature at Mendoza station, Zonda B.

Surface *T*	ERA USGS	GFS USGS	ERA GEAA	GFS GEAA	Ideal value
d-Index	0.89	**0.92**	0.86	**0.94**	1
sdBIAS	−0.77	−0.95	−1.16	**−0.44**	min (abs)
sdisp	4.06	3.36	4.26	**2.99**	min (abs)
MBE	−0.05	**0.00**	0.18	**0.11**	min (abs)
RMSD	−0.61	**−0.52**	−0.77	**−0.52**	min (abs)
RMSE	0.61	**0.52**	0.79	**0.54**	min (abs)

Table 4
Best options selected for zonal wind component (U10), all surface stations, ZA event.

	ZA_MZA		ZA_SJ		ZA_SM		
d-Index	GFS_GEAA		ERA_GEAA	GFS_USGS	ERA_GEAA	GFS_GEAA	ERA_USGS
BIAS	GFS_GEAA		ERA_GEAA		GFS_GEAA		
Disp	GFS_GEAA		GFS_GEAA		GFS_GEAA	ERA_GEAA	
MBE	GFS_GEAA		GFS_USGS		GFS_GEAA		
RMSD	ERA_GEAA		GFS_GEAA		ERA_GEAA	GFS_GEAA	
RMSE	ERA_GEAA	GFS_GEAA	GFS_GEAA		ERA_GEAA	GFS_GEAA	

of 1800 × 2160 km^2 covered west central Argentina including the complex topography of the Andes Mountain Range. The second domain (of 12 km grid cells) covered the Province of Mendoza (centered at 32.9°S, 68.5°W; and an area of 168 × 264 km^2), and the smallest domain (of 4 km grid cells) was used to represent, with a high horizontal resolution, the metropolitan urban zone of Mendoza, San Juan and its rural periphery (centered in 32.8°S, 68.8°W; 84 × 88 km^2).

The model was configured to run from August 23 to August 30, 2010 for the ZA event and from April 16 to April 23, 2011 for ZB, with outputs every hour. With the purpose of providing suitable soil moisture and temperatures, the land surface model was initialized by spinning up the soil properties in the model for 96 h, using the humidity rate of change as criterion for appropriateness.

Sixty sigma vertical levels up to 50 hPa were used. Meteorological continuous simulations, with one single initialization of large-scale fields and frequent updates of lateral boundary conditions, are currently the most common approach in regional simulations. In that sense, two meteorological time-dependent boundary and initial conditions were used: a) NCEP Global Final Analysis of GFS with a resolution of 0.5°, updated every 6 h (UCAR, 2002); and b) ERA Interim from the European Centre for Medium-Range Weather Forecasts (ECMWF), with a resolution of 0.7°, also every 6 h (Dee et al., 2011). Hereafter, for the purpose of results comparison, the first dataset will be referred to as GFS and the second, as ERA.

To describe western Argentina complex terrain geography, high resolution elevation data were included. The WRF Pre-Processing System (WPS) module was modified in order to use data from the Shuttle Radar Topography Mission (SRTM3) (Rodriguez et al., 2005), which improves terrain elevation more than ten-fold with a resolution of 3″ × 3″ (90 m × 90 m) but also contained a better description of the complex terrain in the study area. Previous simulations with SRTM3 data showed overall lower errors when compared to simulations driven with default elevation data, both in terms of wind speed and direction.

The default classification of land use included in the WRF model was developed by the Geological Survey of the United States (USGS) with a resolution of 30″ and with global land cover characteristics based on 24 categories. This land cover database will be named USGS. Since most of Mendoza's urban center, cultivated areas and arid piedmont areas were not well characterized, land cover data from the European Space Agency (ESA) map GLOBCOVER 2009 (Arino et al., 2010; Bontemps et al., 2011) was adapted with a 300 m resolution. This map has 22 land coverage classes defined by the United Nations (UN) in the Land Cover Classification (LCC) System, which were adjusted to fit the USGS classification scheme. A better representation of urban areas was achieved by reallocating LULC characteristics using satellite data from the Operational Linescan System of the Defense Meteorological Satellite Program (DMSP–OLS) of night time lights (NOAA-NGDC, 2010), normally associated with urban occupation. This adjusted LULC database will be called GEAA.

Several options were selected to configure the WRF model (Table 1). Grid-nudging was included in both principal domains for the prediction of wind components using the control coefficients given by default, for all levels outside the PBL, every 6 h consistent with the frequency of both GFS and ERA reanalysis data. No local observed meteorological quantity was inserted into model integration through relaxation forcing terms. Initialization was performed using observed data. This entire configuration was tested in other case studies producing the best estimates of temperature, wind and humidity at surface level than any other configuration on the two studied episodes (Cremades et al., 2011).

3. Results

3.1. Model evaluation

Table 2 summarizes all comparison variants for the WRF model runs. It includes two events (ZA and ZB), 4 runs for each event using 2 reanalysis datasets (GFS or ERA) and 2 databases of land use (USGS or GEAA). At the surface level, the temperature, dew point, zonal and meridional wind component variables (*T*, *DP*, *U10*, *V10*) were evaluated for each event against three Argentinian stations: Mendoza (MZA, 32.83°S, 68.83°W, 704 m), San Juan (SJ, 31.567°S, 68.5°W, 598 m) and San Martín (SM; 33.083°S, 68.5°W, 653 m) and at 11 levels of standard pressure for the same four variables (*T*, *DP*, *U10*, *V10*) for each event against the radiosonde stations of Mendoza (MZA) and Santo Domingo (33.65°S, 71.61°W, 75 m), Chile.

The statistical analysis totalized 144 cases for all surface variables (2 events × 4 parameters × 1 level × 3 stations × 6 statistics) and 1056 cases for upper air variables (2 events × 4 parameters × 11 mandatory pressure levels × 2 stations × 6 statistics. For every case, we compared 4 different configurations (2 reanalysis datasets, 2 LULC databases) to measurements. Surface data were provided by the Servicio Meteorológico Nacional (SMN) [Argentine National Meteorological Service] and upper air data with a 12-hour resolution were obtained from the NOAA/ESRL Radiosonde Database (RAOB). Model agreement to

Table 5
Score assigned to each option according to variables.

Variable	T		DP		U10		V10		Total	
Option	N	%	N	%	N	%	N	%	N	%
GFS USGS	13	23%	13	27%	9	18%	4	9%	39	20%
GFS GEAA	17	30%	17	35%	22	44%	13	30%	69	35%
ERA USGS	12	21%	4	8%	4	8%	8	18%	28	14%
ERA GEAA	14	25%	15	31%	15	30%	19	43%	63	32%
GFS	30	54%	30	61%	31	62%	17	39%	108	54%
ERA	26	46%	19	39%	19	38%	27	61%	91	46%
USGS	25	45%	17	35%	13	26%	12	27%	67	34%
GEAA	31	55%	32	65%	37	74%	32	73%	132	66%
Total score	56	100%	49	100%	50	100%	44	100%	199	100%

Table 6
Grouped results for the scores assigned to each option according to stations and event.

Option	MZA	SJ	SM	ZA	ZB
GFS_USGS	15	17	7	19	20
GFS_GEAA	23	17	29	35	34
ERA_USGS	9	13	6	20	8
ERA_GEAA	21	17	25	29	34
GFS	38	34	36	54	54
ERA	30	30	31	49	42
USGS	24	30	13	39	28
GEAA	44	34	54	64	68
Total score	68	64	67	103	96

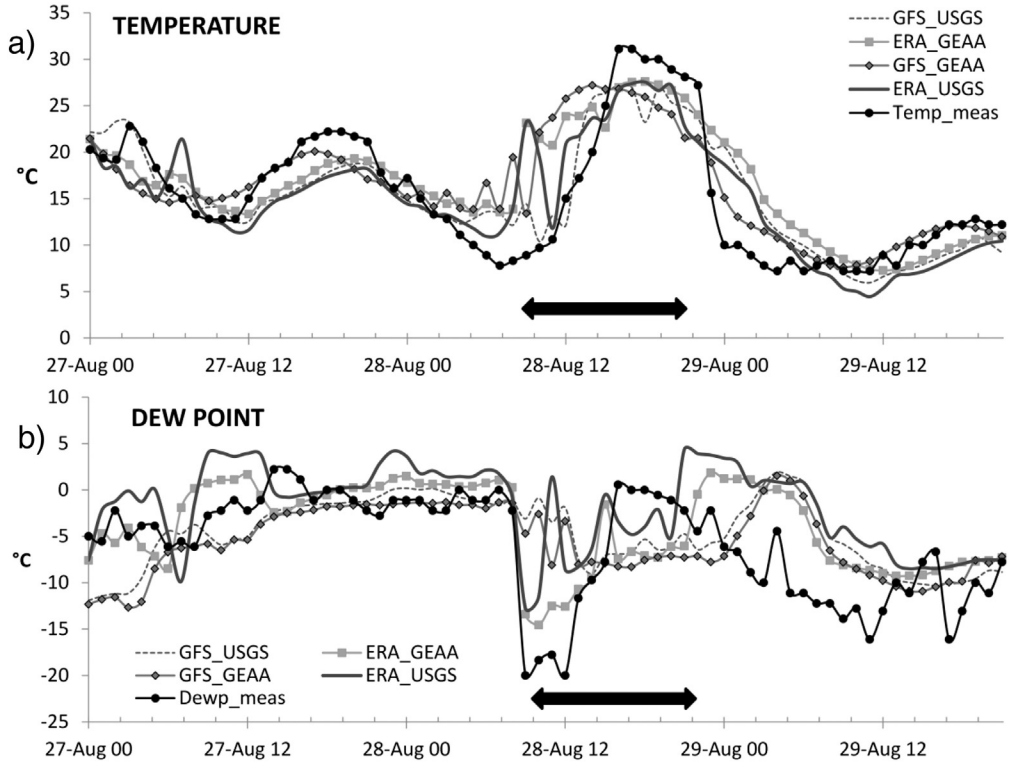

Fig. 5. Measurements at Mendoza station and simulations of the evolution of 2 m-air temperature (a) and 2 m-dew point temperature (b) for the Zonda event on August 28, 2010 as well as the previous and the following days.

measurements was evaluated using several performance statistics: Mean Bias Error (MBE), Root Mean Square Error (RMSE), Mean Absolute Error (MAE), Willmott's Index of Agreement (d-index), Linear correlation coefficient (r), Unbiased Root Mean Square Difference (RMSD), Variability error (BIAS) and Dispersion Error (disp). However, since many coefficients deliver similar information (Takacs, 1985; Hou

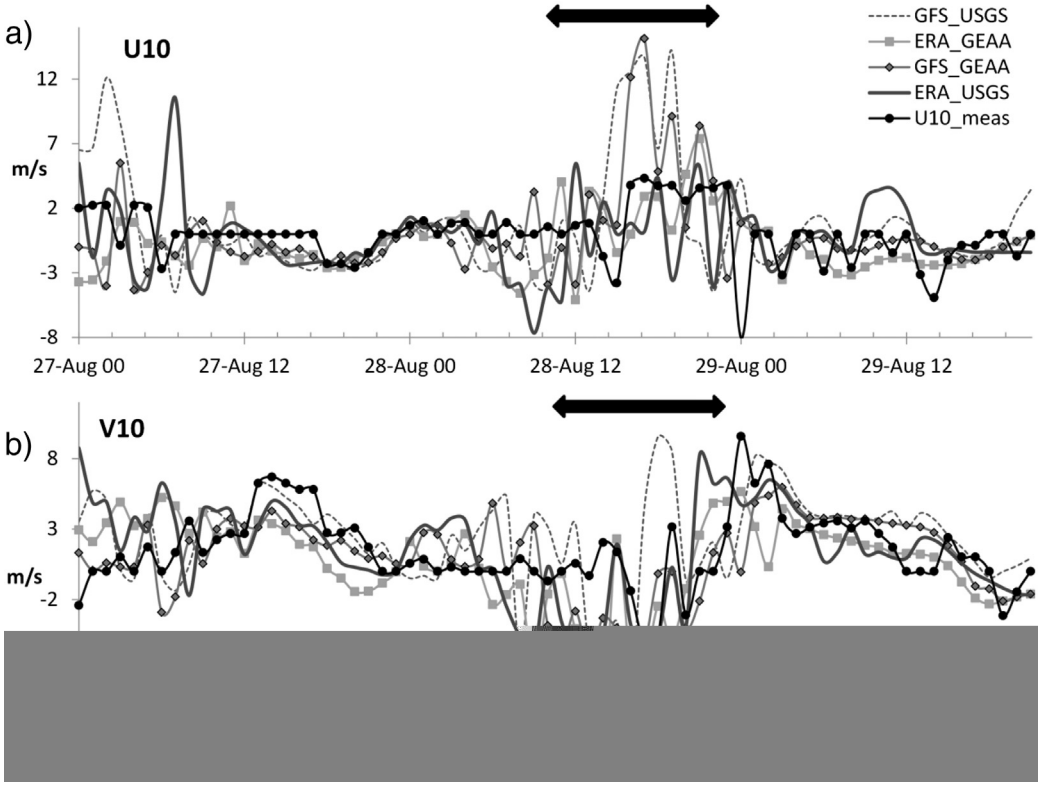

Fig. 6. Measurements at Mendoza station and simulations of the evolution of zonal wind component (u10) (a) and meridional wind component (v10) (b) for the Zonda event on August 28, 2010 as well as the previous and the following days.

Table 7
Score given to each option in relation to temperature in both stations.

Option	Low levels	Medium-low levels	Medium-high levels	High levels	Total
GFS_USGS	11	29	24	31	95
GFS_GEAA	10	17	11	16	54
ERA_USGS	12	13	20	18	63
ERA_GEAA	3	18	28	18	67
GFS	21	46	35	47	149
ERA	15	31	48	36	130
USGS	23	42	44	49	158
GEAA	13	35	39	34	121
Total score	36	77	83	83	279

Table 8
Score given to each option for all variables according to pressure levels.

Option	Low levels	Medium-low levels	Medium-high levels	High levels	Total
GFS_USGS	29	105	84	61	279
GFS_GEAA	39	69	87	44	239
ERA_USGS	40	71	104	72	287
ERA_GEAA	36	58	115	50	259
GFS	68	174	171	105	518
ERA	76	129	219	122	546
USGS	69	176	188	133	566
GEAA	75	127	202	94	498
Total score	144	303	390	227	1064

et al., 2001; Lange, 2005; Banerjee et al., 2011; Ritter et al., 2013; Wilks, 2011; Willmott et al., 2012), MBE, RMSD, RMSE, disp, BIAS and d-index were selected as indicators of precision, accuracy and performance. A detailed description of the selected statistics and their relation with the model performance can be found in Appendix A.

In order to assess the behavior of the model, the best performances for each variable and performance statistic were selected and the best performing parameter combinations were assigned one point (for instance, MBE of surface *T* for ZA in Mendoza, using GFS and USGS). If, for a specific variable, more than one option generated outputs representing an equally good agreement with observations, one point was assigned to each of these options. All points were then summed and the relative weights for each option were evaluated (See Appendix B, for a more detailed explanation). From surface comparisons we actually obtained 199 valid configurations, for the 144 cases and for the upper air analysis, a total of 1064 valid configurations were obtained for the 1056 cases.

3.2. Evaluation of surface variables

Output comparison of the WRF model to surface observations was performed in meteorological stations of MZA, SM and SJ airports for both ZA and ZB Zonda episodes.

Table 3 shows an example of the results obtained for surface temperature in Mendoza station, with a detailed account of precision and accuracy errors as well as Willmott's performance index (all other variables at the other stations for all events are shown in Appendix B).

In order to exemplify score assignment, it is observed that, in Table 3, the GFS USGS and GFS GEAA options obtained the best indicator for d-Index, and one point was assigned to each specific combination of parameters. The same procedure was followed for all runs and variables.

Table 4 shows as an example the best parameter combinations for zonal wind component (*U10*) using all surface stations for Zonda A case. Table 5 summarizes the results for all surface variables, divided into three sub tables; on top, results for each parameter combination of reanalysis dataset and soil use, GFS USGS, GFS GEAA, ERA GEAA, are shown; in the second sub table results are grouped according to whether reanalysis were GFS or ERA (regardless of land use); and in the third sub table, results are grouped according to land use, be it USGS or GEAA (regardless of whether the reanalysis used was GFS or ERA).

Table 6 groups results according to the surface station considered (both Zondas) and in the last columns for each Zonda individually for all surface stations.

Figs. 5 and 6 show the observed and simulated temporal evolution of temperature, dew point temperature and surface wind components for the August 28 Zonda episode (ZA). In Fig. 5, a rise of temperature at 2 m and a clear drop of the dew point temperature can be observed. Several hours after the Zonda event, meteorological values regain monthly typical values reported by SMN. It is possible to observe that, for surface temperature, the model presents slight tendencies to overestimation, though magnitude depends on the simulated event. Studies performed

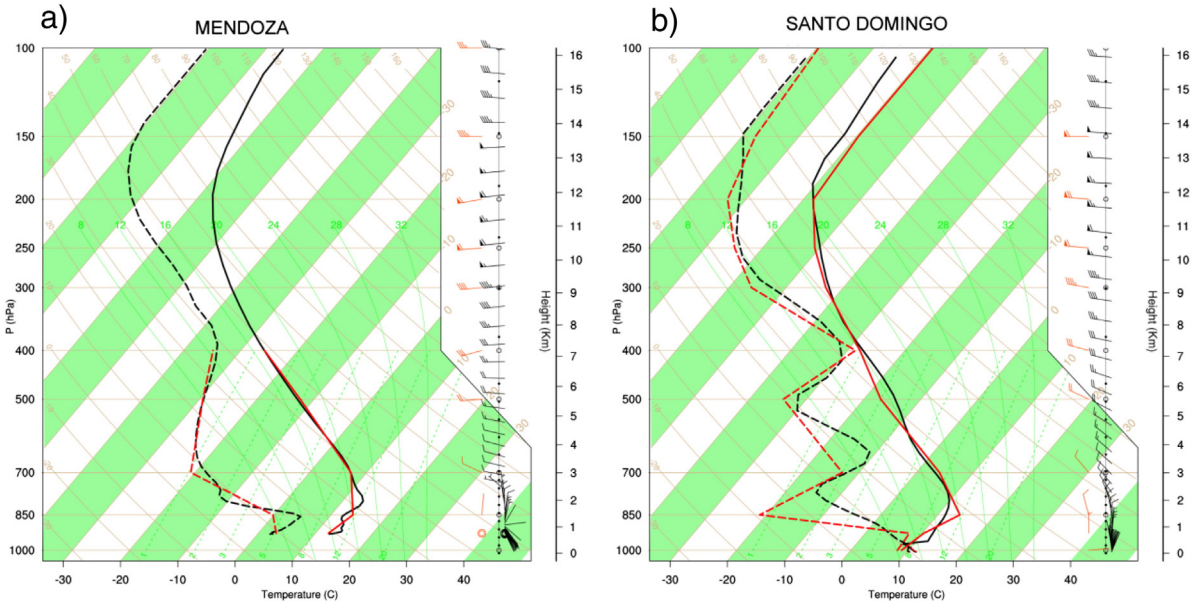

Fig. 7. Skew-T diagrams showing the temperature and dew point profiles and the simulated and measured wind profiles for the Zonda event of April 21, 2011 at 12Z, with the ERA USGS configuration: a) measured in MZA station; b) measured in Santo Domingo station. The values measured taken from the NOAA/ESRL Radiosonde Database are shown in black. The values simulated with WRF are shown in red. (For interpretation of the references to color in this figure legend, the reader is referred to the web version of this article.)

Table 9
Score given to each option for all variables in both upper-air stations (Mendoza and Santo Domingo).

Variable	T		DP		U10		V10		Total
Option	N	%	N	%	N	%	N	%	N
GFS_USGS	95	34%	51	22%	70	25%	63	23%	279
GFS_GEAA	54	19%	46	20%	71	25%	68	24%	239
ERA_USGS	63	23%	58	26%	80	29%	86	31%	287
ERA_GEAA	67	24%	72	32%	59	21%	61	22%	259
GFS	149	53%	97	43%	141	50%	131	47%	518
ERA	130	47%	130	57%	139	50%	147	53%	546
USGS	158	57%	109	48%	150	54%	149	54%	566
GEAA	121	43%	118	52%	130	46%	129	46%	498
Total score	279	100%	227	100%	280	100%	278	100%	1064

in other latitudes have shown deviations between −5 K and 4 K (Ashrit and Mohandas, 2010; Das et al., 2008) while in our work, magnitude errors are less than 1 K, according to the MBE estimations for all stations (MBE = -0.18 ± 0.65). Likewise, Fig. 6 shows the observed and simulated temporal evolution of the wind components for the same event.

The Zonda (ZA) event had a severe intensity, with estimated gustiness of up to 40 m/s, and predominantly W-NW winds during the episode. Although different tested configurations show a variable performance depending on the simulated period, in this case, that the model tends to overestimate speeds, though to a lesser extent for the GFS GEAA and ERA GEAA configurations (see Appendix C, for more detailed descriptions of these simulation results). In that sense, MBE decreases by 57% on average for U10 and V10 with respect to its respective variants that use the default land use data (USGS). Similar results have been observed in previous studies (Ruiz et al., 2010). It's worth noting that wind speed is generally strongly influenced by local variations, particularly when these include severe instability conditions (Nielsen-Gammon et al., 2010) like Zonda events.

3.3. Evaluation of upper air variables

The evaluation of the WRF model performance in relation to upper air variables was carried out by comparing it with two radiosonde stations within the study domain, one in Mendoza (Argentina) on the eastern slope of the Andes mountain range (32.83°S, 68.83°W, 704 m), and the second one in Santo Domingo (Chile) on the western slope of the Andes (33.65°S, 71.61°W, 75 m). Four variables (*T*, *DP*, *U10*, and *V10*) were evaluated at 11 mandatory pressure levels using the same scheme used for surface data. In order to summarize the information, vertical levels were grouped as follows: a) Low levels (1000 and 925 hPa); b) Medium-low levels (850, 700 and 500 hPa); c) Medium-high levels (400, 300 and 250 hPa); and d) High levels (200, 150 and 100 hPa) (Table 7).

Fig. 7 shows a comparison between the values observed and the simulations for the best performing configuration, according to the data in Table 8, for upper air variables on the date of the ZB event at 1200 UTC. In addition, it can be observed that deviations get slightly larger as height increases. The differences in dew point temperature are higher; however, in general, there is a clear correspondence between measurements and observations in all cases. In general, an overestimation by the model can be observed in medium-low levels and medium-high levels. In relation to winds, the best results are seen in high levels and medium-high levels, both in terms of direction and speed. At low-levels, deviations are larger and the model performance shows a much higher variability with each configuration.

Finally, a summary of the scores according to pressure levels in the evaluation of upper air variables is presented in Table 8 (details on the scores for all configurations and all upper air variables can be found in Appendix D). In the same way, Table 9 shows a summary of the scores for all variables and configurations for both upper-air stations.

Table 10 provides a qualitative summary of the results, where a total of 10 stars (*) per variable, both for surface and upper air, were assigned. Each Option received a percentage of the correct predictions shown in Tables 5 and 9. In this sense, GFS GEAA yielded better surface results, and it also proved to be an acceptable upper air configuration, together with other options. In addition, the ERA GEAA configuration performed well on surface.

Table 10
Qualitative classification of options.

Surface	*GFS USGS*	*GFS GEAA*	*ERA USGS*	*ERA GEAA*
Temperature 2 m	**	***	**	***
Dew temperature 2 m	**	****	*	***
U10	**	****	*	***
V10	*	***	*	*****
Total	7	14	5	14
Upper air	*GFS USGS*	*GFS GEAA*	*ERA USGS*	*ERA GEAA*
Temperature	****	**	**	**
Dew temperature	**	**	***	***
U	**	***	***	**
V	**	***	***	**
Total	10	10	11	9
Surface + Upper air	*GFS USGS*	*GFS GEAA*	*ERA USGS*	*ERA GEAA*
Total	17	24	16	23

Each variable (row) recieves 10 asterisks which are distributed according to percentage assigned in Table 5 and Table 9 (see text).

4. Discussion and conclusions

This study showed the results of a simulation of two Zonda events using the WRF model in a mountain area with a complex terrain, in this case, the Andes Mountain Range. The objective was to study the effect of using several time-updated boundary conditions for reanalysis and datasets of LULC in greater or lower detail. The model was thus run using a combination of such databases and results were compared to meteorological data provided by surface and upper air (radiosonde) weather stations in the study area, generally located in the most important urban centers of western-central South America. In order to evaluate the multiple surface and upper air variables, a scoring system analyzing the performance of the MBE, RMSE, BIAS, disp, RMSD and d-index statistics was proposed. It must be noted that, in assigning a point to the best option, the difference between one option and another may be very small and, therefore, the number of cases evaluated becomes important in order to obtain a representative statistic and to discover a behavior pattern for the model. Consequently, if two configurations showed similar results, better than the rest, both options were considered as the best.

Tables 5 and 6 show that GFS GEAA would be the best option for all surface stations. However, when variables are analyzed individually, the best option for temperature is GEAA, although no large differences were observed in using either GFS or ERA. With regard to surface dew point temperatures, results are similar and the use of a locally adapted LULC configuration seemed to improve the description of this variable by the WRF model. For the U10 wind component, the best option is GFS GEAA. On the other hand, for the meridional component, although the GFS GEAA configuration showed good results, the best option was ERA GEAA. The Mendoza and San Juan stations were best represented with GFS GEAA for all variables, and the San Martín station, with ERA GEAA. Regardless of the reanalysis used, these results seem to confirm that a better representation of LULC improved the WRF model's ability to predict surface variables, regardless of the type of environment: both in the structure of narrow valleys surrounded by hills in the city of San Juan and the surrounding cultivated area, and in the arid piedmont and the prominently urban area of Mendoza. In all cases, simulations using GFS slightly improved the results compared to ERA.

The MBE indicates the level of overestimation and underestimation of each simulation with the different model configurations. In this

sense, in terms of temperature, simulations overerestimated observations with all configuration options, although to a greater extent when the default land use (USGS) was used. Almost all simulations overestimated the dew point temperature values, regardless of the configuration being used. The model slightly overestimated both wind components with any configuration although the use of ERA data and GEAA configurations slightly improved the prediction.

The best option for the evaluation of upper air variables (see Table 8) was ERA USGS although GFS USGS and ERA GEAA also seemed to be acceptable configurations. In addition, ERA yielded a larger number of correct predictions than GFS for the higher levels, while GFS seemed to better represent the variables at medium-low levels. In low levels, ERA had better results, but with small differences in relation to GFS. It is worth noting that at lower levels, the amount of valid data to perform the statistical comparisons is variable, since the upper air station in Mendoza is located at 704 m a. m. s. l. and the Santo Domingo station is near the Pacific Ocean. The detail of land use loses influence as height increases. As from 300 mbar, most correct predictions alternate between both initial conditions, USGS-GEAA and GFS-ERA. GFS USGS reported the best upper air results for *T* and ERA GEAA for *DP* (see Table 9), while *U10* and *V10* were best described by ERA USGS.

Regarding upper air, several configurations described the Zonda events similarly however, if a global evaluation were to be conducted, the GEAA configurations would best represent the characteristics of the mountain area under study. This study showed that GFS GEAA yields more uniform results both on the surface and in the upper air except for temperature and dew point, particularly at low levels. It should be noted that the proposed scoring system intents to provide a uniform evaluation scheme for all variables which will integrate different kinds of information and which is valid for all the cases under study.

Acknowledgments

Authors would like to acknowledge ESA for providing GlobCover 2009 (© ESA 2010 & UC Louvain) datasets. This work was supported by the National Scientific and Technical Research Council (CONICET), Universidad Tecnológica Nacional (UTN) of Argentina, under Grant Project # PID UTN IFI1487 Cod. 25/JC01 and PIP CONICET # 112 20110100673 and PICT 2012-1021.

Appendix A. Supplementary data

Supplementary data to this article can be found online at http://dx.doi.org/10.1016/j.atmosres.2015.06.011.

References

Arino, O., Ramos, J., Kalogirou, V., Defoumy, P., Achard, F., 2010. GlobCover 2009. ESA Living Planet Symposium, Bergen, Norway, p. 686.
Ashrit, R., Mohandas, S., 2010. Mesoscale model forecast verification during monsoon 2008. J. Earth Syst. Sci. 119 (4), 417–446.
Banerjee, T., Singh, S.B., Srivastava, R.K., 2011. Development and performance evaluation of statistical models correlating air pollutants and meteorological variables at Pantnagar, India. Atmos. Res. 99 (3–4), 505–517.
Bontemps, S., Defourny, P., Van Bogaert, E., Arino, O., Kalogirou, V., Ramos Perez, J., 2011. GLOBCOVER 2009 Products Description and Validation Report. http://due.esrin.esa.int/globcover/LandCover2009/GLOBCOVER2009_Validation_Report_2.2.pdf (Accessed 21 Oct 2014).
Borque, P., Salio, Paola, Nicolini, Matilde, et al., 2010. Environment associated with deep moist convection under SALLJ conditions: a case study. Weather Forecast. 25, 970–984.
Carvalho, D., Rocha, A., Gómez-Gesteira, M., Santos, C., 2012. A sensitivity study of the WRF model in wind simulation for an area of high wind energy. Environ. Model. Softw. 33, 23–34.
Cremades, P.G., Puliafito, Salvador Enrique, Allende, D.G., Fernandez, R.P., 2011. An approach for using remote sensing products and ground observations in the evaluation of a Numerical Weather Prediction model. In: Möller, O., Signorelli, J.W., Storti, M.A. (Eds.), Mecánica Computacional vol. XXX. AMCA, Rosario, Argentina, pp. 3529–3542.
Das, S., Ashrit, R., Iyengar, G.R., Mohandas, S., Gupta, M. Das, George, J.P., Dutta, S.K., 2008. Skills of different mesoscale models over Indian region during monsoon season: forecast errors. J. Earth Syst. Sci. 5, 603–620.
Dee, D.P., Uppala, S.M., Simmons, A.J., et al., 2011. The ERA-Interim reanalysis: configuration and performance of the data assimilation system. Quarterly Journal of the Royal Meteorological Society 137(656). John Wiley & Sons, Ltd., pp. 553–597.
DuVivier, A.K., Cassano, J.J., 2012. Evaluation of WRF model resolution on simulated mesoscale winds and surface fluxes near Greenland. Mon. Weather Rev. 141, 941–963.
Ezcurra, A., Benech, B., Echelecou, A., Santamaría, J.M., Herrero, I., Zulueta, E., 2013. Influence of local air flow regimes on the ozone content of two Pyrenean valleys. Atmos. Environ. 74, 367–377.
Hou, D., Kalnay, E., Droegemeier, K.K., 2001. Objective verification of the SAMEX '98 ensemble forecasts. Mon. Weather Rev. 129 (1), 73–91.
Jiménez, P.A., González-Rouco, J.F., García-Bustamante, E., Navarro, J., Montávez, J.P., de Arellano, J.V.-G., Dudhia, J., Muñoz-Roldan, A., 2010. Surface wind regionalization over complex terrain: evaluation and analysis of a high-resolution WRF simulation. J. Appl. Meteorol. Climatol. 49, 268–287.
Kaltenboeck, Rudolf, Steinheimer, Martin, 2014. Radar-based severe storm climatology for Austrian complex orography related to vertical wind shear and atmospheric instability. Atmospheric Research. Elsevier (Available online 27 August 2014).
Lange, M., 2005. On the uncertainty of wind power predictions—analysis of the forecast accuracy and statistical distribution of errors. J. Sol. Energy Eng. 127 (2), 177.
Lee, J., Shin, H.H., Hong, S., Jiménez, P.A., Dudhia, J., Hong, J., 2015. Impacts of subgrid-scale orography parameterization on simulated surface layer wind and monsoonal precipitation in the high-resolution WRF model. J. Geophys. Res. Atmos. 120, 644–653.
Mesinger, F., Jovic, D., Chou, S.C., Gomes, J.L., Bustamante, J.F., 2006. Wind forecast around the Andes using the sloping discretization of the Eta coordinate. Proceedings Eight Int. Conf. on the Southern Hemisphere Meteorology and Oceanography, Foz de Iguazu, INPE, pp. 1837–1848.
Michalakes, J., Dudhia, J., Gill, D., Henderson, T., Klemp, J., Skamarock, W., Wang, W., 2004. The Weather Research and Forecast Model: Software Architecture and Performance.
Mira-Salama, D., Van Dingenen, R., Gruening, C., Putaud, J.-P., Cavalli, F., Cavalli, P., Erdmann, N., Dell'Acqua, A., Dos Santos, S., Hjorth, J., Raes, F., Jensen, N.R., 2008. Using Föhn conditions to characterize urban and regional sources of particles. Atmospheric Research 90(2–4). Elsevier B.V., pp. 159–169.
Nicolini, Matilde, García, Yanina, 2011. Diurnal cycle in convergence patterns in the boundary layer east of the Andes and convection. Atmospheric Research 100(4). Elsevier B.V., pp. 377–390.
Nielsen-Gammon, J.W., Hu, X.-M., Zhang, F., Pleim, J.E., 2010. Evaluation of planetary boundary layer scheme sensitivities for the purpose of parameter estimation. Mon. Weather Rev. 138 (9), 3400–3417.
NOAA-NGDC, 2010. Version 4 DMSP-OLS Nighttime Lights Time Series. http://www.ngdc.noaa.gov/dmsp/downloadV4composites.html.
Norte, F., 1988. Características del viento Zonda en la Región de Cuyo. Universidad de Buenos Aires.
Norte, F., Ulke, A., Simonelli, S., Viale, M., 2008. The severe Zonda wind event of 11 July 2006 east of the Andes Cordillera (Argentine): a case study using the BRAMS model. Meteorog. Atmos. Phys. 102, 1–14.
Papanastasiou, D.K., Melas, D., Lissaridis, I., 2010. Study of wind field under sea breeze conditions; an application of {WRF} model. Atmos. Res. 98, 102–117.
Ritter, Mathias, Müller, Mathias D., Tsai, Ming-Yi, et al., 2013. Air pollution modeling over very complex terrain: an evaluation of WRF-Chem over Switzerland for two 1-year periods. Atmospheric Research 132–133. Elsevier B.V., pp. 209–222.
Rodriguez, E., Morris, C.S., Belz, J.E., Chapin, E.C., Martin, J.M., Daffer, W., Hensley, S., 2005. An assessment of the SRTM topographic products. Technical Report JPL D-31639. Pasadena, California.
Ruiz, J.J., Saulo, C., Nogués-Paegle, J., 2010. WRF model sensitivity to choice of parameterization over South America: validation against surface variables. Mon. Weather Rev. 138 (8), 3342–3355.
Santos-Alamillos, F.J., Pozo-Vázquez, D., Ruiz-Arias, J.A., Tovar-Pescador, J., 2015. Influence of land-use misrepresentation on the accuracy of {WRF} wind estimates: evaluation of {GLCC} and {CORINE} land-use maps in southern Spain. Atmos. Res. 157, 17–28.
Seluchi, M.E., Norte, F.A., Satyamurty, P., Chou, S.C., 2003. Analysis of three situations of the Foehn effect over the Andes (Zonda Wind) using the Eta–CPTEC regional model. Weather Forecast. 18, 481–501.
Skamarock, W.C., Klemp, J.B., Gill, D.O., Barker, D.M., Wang, W., Powers, J.G., 2008. A Description of the Advanced Research WRF Version 3. Mesoscale and Microscale Meteorology Division, National Centre for Atmospheric Research.
Sun, Wen-Yih, 2013. Numerical study of severe downslope windstorm. Weather and Climate Extremes 2. Elsevier, pp. 22–30.
Takacs, L.L., 1985. A two-step scheme for the advection equation with minimized dissipation and dispersion errors. Mon. Weather Rev. 113, 1050–1065.
UCAR, 2002: University Corporation for Atmospheric Research, U.S. National Centers for Environmental Prediction, and E. C. for M.-R. W. F. European Centre for Medium-Range Weather Forecasts University Corporation for Atmospheric Research [Unidata], U.S. National Centers for Environmental Prediction, 2002: Dataset ds335.0 published by the CISL Data Support Section at the National Centre for Atmospheric Research. http://dss.ucar.edu/datasets/ds335.0/.
Viale, M., Nuñez, M.N., 2010. Climatology of winter orographic precipitation over the subtropical Central Andes and associated synoptic and regional characteristics. J. Hydrometeorol. Am. Meteorol. Soc. 12 (4), 481–507.
Wilks, D.S., 2011. Chapter 9—Time Series. In: Daniel, S., Wilks, B.T. (Eds.), Geophysics, InternationalStatistical Methods in the Atmospheric Sciences. Academic Press, pp. 395–456.
Willmott, C.J., Robeson, S.M., Matsuura, Kenji, 2012. A refined index of model performance. International Journal of Climatology 32(13). John Wiley & Sons, Ltd., pp. 2088–2094.
Zydek, F., 2000. Chinook wind. South Dakota Rev. 38 (1), 54.